# CHAPTER 7

# PARAMETER STUDY ON STEEL FIBRE REINFORCED CONCRETE GROUND SLABS

## 7.1 Introduction

A parameter study is conducted to investigate the influence of concrete strength, steel fibre content and the support stiffness on the *P-Δ* response of SFRC ground slabs. The parameter analysis is conducted by changing parameters either on the tensile $\sigma$-$\varepsilon$ curve or on the support material model. The *P-Δ* responses are calculated using the finite element model presented in chapter 6. In the analysis, only one parameter will be changed at a time while keeping the other parameters fixed. The study will serve as an aid in adjusting the materials used when designing SFRC ground slabs and give an insight into the behaviour of the SFRC ground slabs. The potential for ultra-thin SFRC ground slabs will also be investigated by analysing a relatively thin SFRC slab.

## 7.2 Models for the SFRC ground slabs

Hypothetical SFRC slabs measuring 3000 x 3000 x 100 mm are assumed for the parameter study. The support was made of typical pavement materials. In the last two analyses, the thickness of the SFRC ground slab is changed to 50 mm to study the possibility for ultra-thin SFRC slabs. The depth of the support was assumed to be 150 mm for all the analyses. Table 7-1 shows the various support materials used in the analyses performed in this chapter. The codes C2, G5, G6 and G9 follow the classification for the South African road building materials. The values in Table 7-1 are either estimated or adapted from the study conducted by Theyse et al. (1996). The cohesion and the angle of friction served as inputs to the Drucker-Prager criterion used for the support material. Poisson’s ratio was assumed to be 0.35 for all the support materials used here.

Table 7-1: Materials used for the support layer.

| Classification | Young’s modulus (MPa) | Cohesion (MPa) | Angle of internal friction |
|---|---|---|---|
| **C2** | 500 MPa | 0.223(*) | 5.50 (*) |
| **G5** | 250 MPa | 0.143 | 3.60 |
| **G6** | 150 MPa | 0.103 | 2.88 |
| **G9** | 50 MPa | 0.1(*) | 1.60 (*) |

(*) Estimated values

The SFRC slabs were centrally loaded by using a steel plate measuring 75 x 75 mm. The size of the loading plate is chosen so that the quarter of the plate fits the size of the finite elements on the symmetry planes. This is to avoid the complexities related to the use of trapezium and the smaller elements when adapting the finite element mesh to the size of the loading plate (refer to section 6.3.1).

Figure 7-1 shows the finite element mesh and the boundary conditions for quarter of the hypothetical slab. The mesh was kept unchanged for all the analyses. Several $\sigma$-$\varepsilon$ responses were used in the analyses. The $\sigma$-$\varepsilon$ response developed in section 5.3 is used in some of the analyses while assumed responses were used for the remainder of the analyses. The rest of the details of the finite element model are kept the same as explained in section 6.3. The $P$-$\Delta$ responses at the loaded point were compared to study the effect of the changed parameters. The $P$-$\Delta$ responses were computed from the consecutive increments by plotting the displacements against four times the reaction of the loaded node.

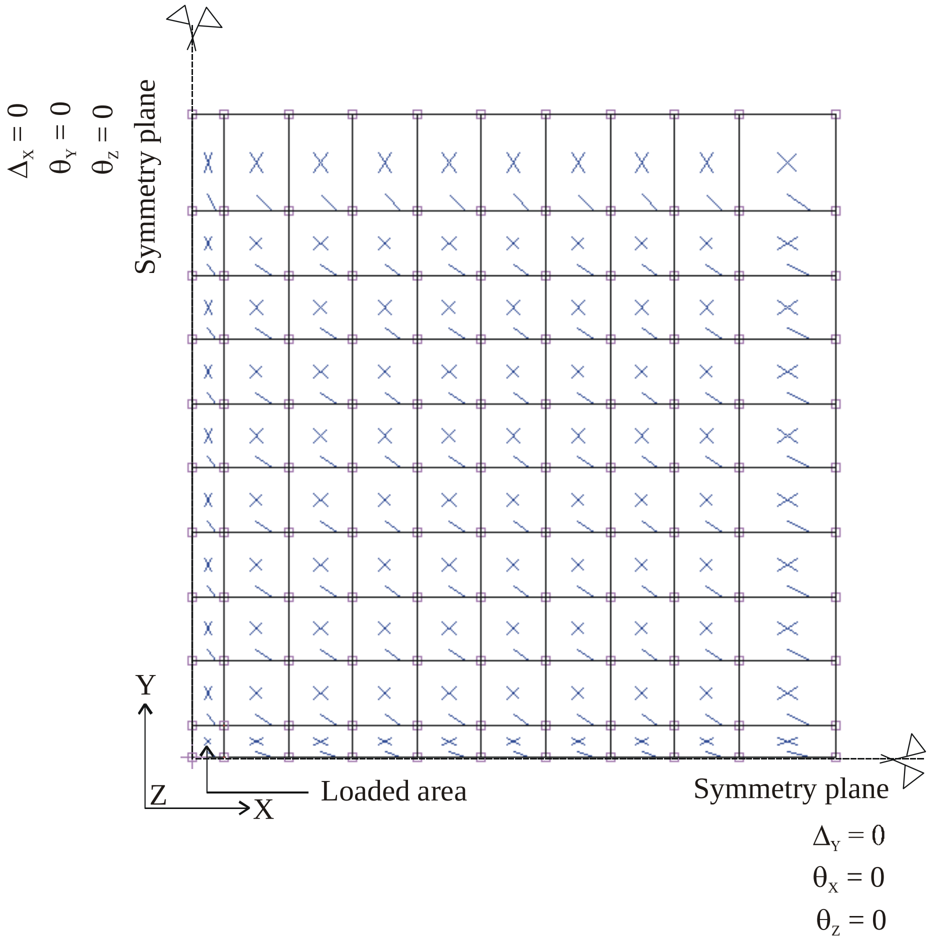


Figure 7-1: The mesh and the boundary conditions for the hypothetical SFRC slab.

### 7.3 Effect of changing strength of concrete

Figure 7-2 shows two tensile *σ-ε* curves for SFRC where only the tensile and compressive strengths are changed. Changing the strength of concrete influences the Young's modulus and the elastic strain. Only the effect due to the change in the Young's modulus is studied here. The possible change in the value of the cracking strain is deemed to be limited and therefore not considered. The *σ-ε* response representing the 45 MPa SFRC is similar to the model calculated for SFRC containing 15 kg/m$^3$ of steel fibres (refer to chapter 5). The *σ-ε* response representing the 75 MPa SFRC is arbitrarily assumed. The increase in the strength of the concrete is expected to increase the post-cracking strength. For the purpose of this analysis, this effect is assumed to be limited only to the first part of the softening curve in the *σ-ε* response. For the support, G9 material is used (refer to Table 7-1). The thickness of the slab used in these analyses is 100 mm.

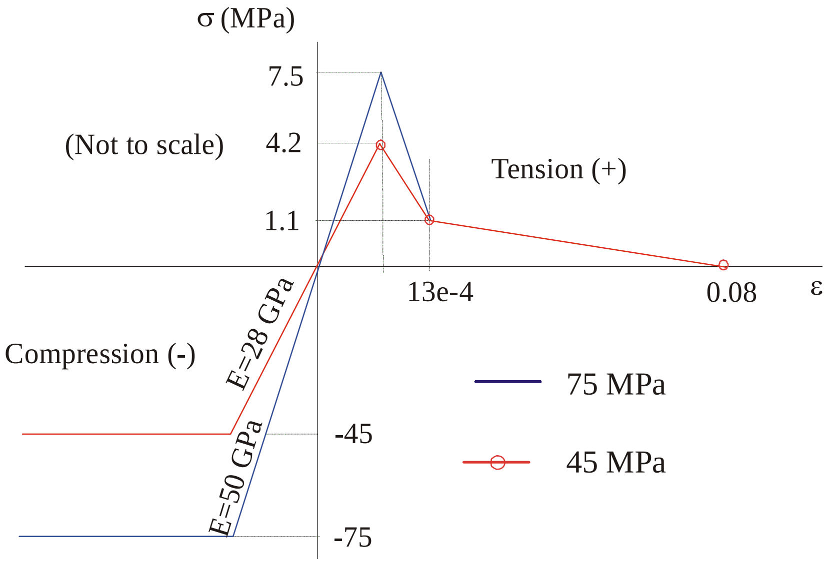


Figure 7-2: Stress-strain curves - changing strength of SFRC.

Figure 7-3 shows that an increase in tensile and compressive strength, results in an increase in the load-carrying capacity of the SFRC ground slabs. For example, at a displacement of 4 mm in the *P-Δ* responses, the load is increased by approximately 39 percent due to an increase of 67 percent in the strength of the concrete (from 45 MPa to 75 MPa). The improvement in the load-carrying capacity is greater at higher displacements than for lower displacements. It also reduces the vertical displacements for equal loads. This is especially useful for thin concrete pavements for which erosion of the support, as the result of excessive deflection, dominates the failure (Canadian Portland Cement Association, 1999).

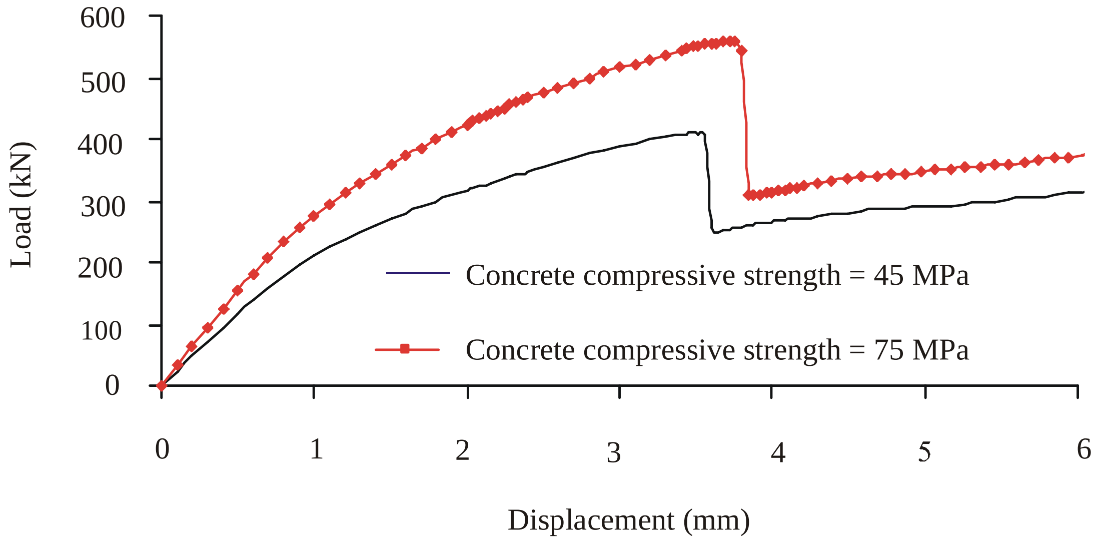


Figure 7-3: Effect of changing strength on load-displacement responses.

## 7.4 Effect of changing steel fibre content

Changing the steel fibre content results in changing the post-cracking strength of the SFRC. This influences the slopes of the softening part of the $\sigma$-$\varepsilon$ curve. Figure 7-4 shows the $\sigma$-$\varepsilon$ responses used in the analysis. For the support, G9 material is used (refer to Table-7-1). The $\sigma$-$\varepsilon$ response representing the 45 MPa SFRC is similar to the model calculated for SFRC containing 15 kg/m$^3$ of steel fibres (refer to chapter 5). The $\sigma$-$\varepsilon$ response for approximately 65 kg/m$^3$ of similar steel fibres is estimated based on the trends shown in Table A-1 (refer to Appendix A). The thickness of the slab used for these analyses is 100 mm.

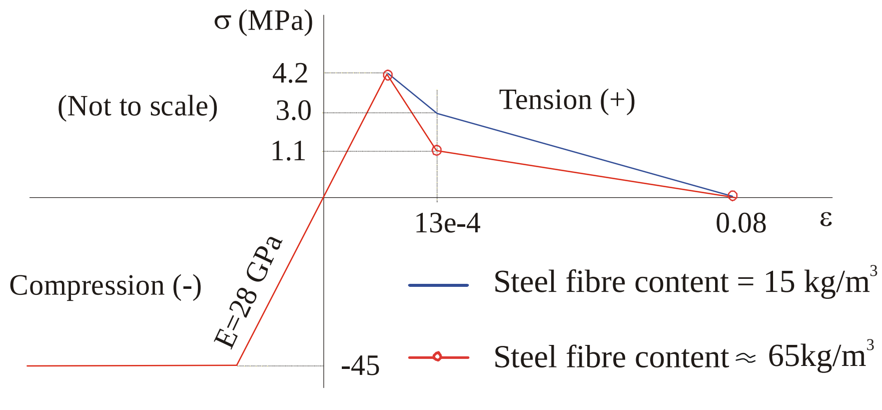


Figure 7-4: Stress-strain curves for SFRC - changing the steel fibre content.

Figure 7-5 indicates that increasing the steel fibre content increases the load-carrying capacity of the SFRC ground slab. It also improves the ductility of the SFRC slab. The SFRC slab with a higher steel fibre content sustained the maximum load for greater displacement values. The analysis showed that the increase in the load-carrying capacity, due the increase in steel fibre content, is significant. At a deflection of approximately 3.5 mm, the addition of extra steel fibres results in approximately 21 percent improvement in the load-carrying capacity. The increase in the percentage of the steel fibre content does not mean an increase of similar percentage in the load-carrying capacity of the SFRC slab. However, the presence of the steel fibres in ground slabs was shown to increase the load-carrying capacity compared to plain concrete slabs. This was demonstrated by many full-scale experiments comparing SFRC and plain concrete ground slabs (refer to section 2.5 and Figure 2-4).

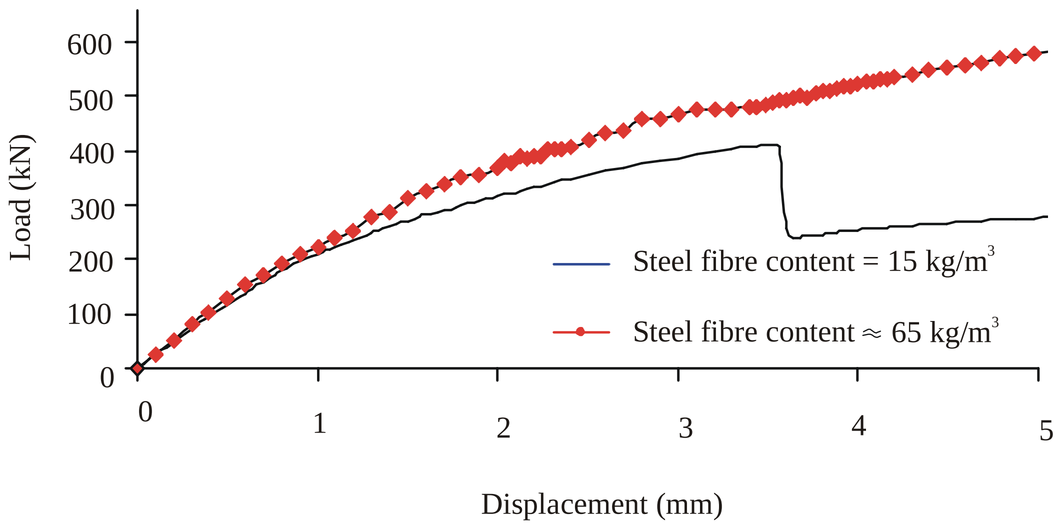


Figure 7-5: Effect of changing steel fibre content on the load-displacement responses.

This influence of the increase in the steel fibre content was also proven from the experimental investigation carried out by Elsaigh and Kearsley (2006). In the investigation, two steel fibre contents of 35 and 65 kg/$m^3$ were added to three concrete mixtures designed to yield cube compressive strengths of 35, 65 and 95 MPa. Three SFRC beams were manufactured for each mixture and loaded at their third-points after 28 days of water curing. The measured $P$-$\delta$ responses are shown in Figure 7-6. These results indicate that increasing the steel fibre content dosage by approximately 86 percent (from 35 to 65 kg/$m^3$) led to insignificant improvement in the post-cracking strength for the beams having a compressive strength of 35 MPa. However, the increase is shown to be significant for beams with a compressive strength of 65 MPa. Increasing the compressive strength to 95 MPa caused the beams to disintegrate immediately beyond the peak load. This is because there were not enough steel fibres across the crack to sustain the peak load attained. The results of this investigation showed that for every concrete compressive strength, a range of useful steel fibre contents exists. Steel fibre content falling out of this range will have no or little contribution to the post-cracking strength of SFRC. Therefore, adding a relatively high steel fibre content to normal strength concrete or adding a relatively low steel fibre content to high strength concrete is a waste of materials. Within the range of the useful steel fibre contents, an increase in steel fibre content will result in an increase in the post-cracking strength. The upper bound of the useful range of steel fibre content will be named as the optimum steel fibre content. The optimum steel fibre content may differ for different types of steel fibres and different concrete strength. This is because differences in the parameters of the steel fibres and matrix strength result in different fibre-matrix characteristics that affect the *P-Δ* response. This should also be considered when evaluating the effect of concrete strength on the *P-Δ* response (refer to section 7.3).

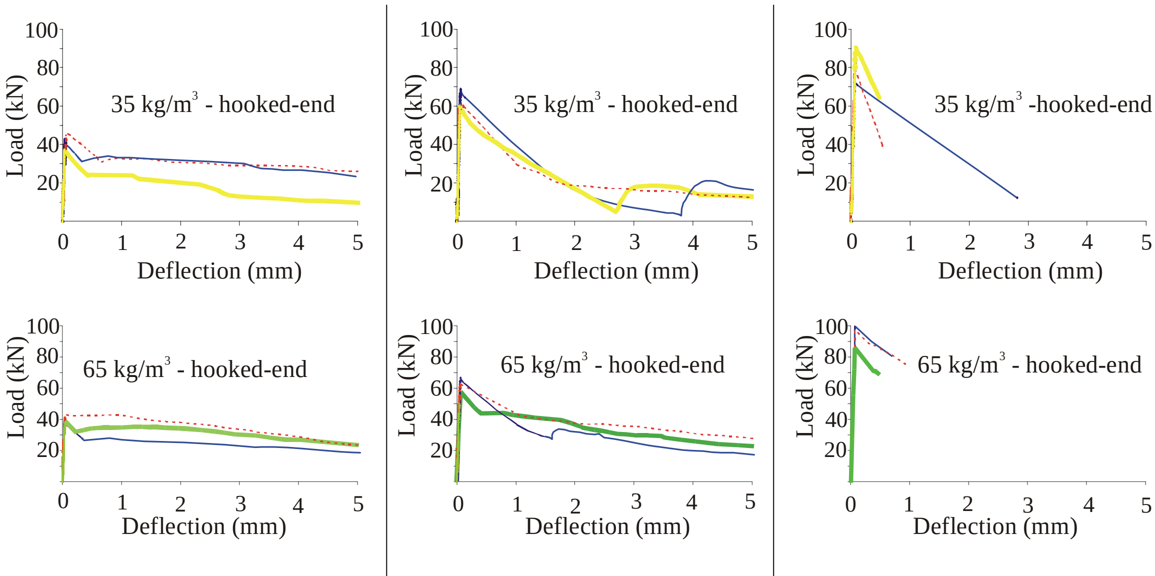


(a) Compressive strength = 35 MPa (b) Compressive strength = 65 MPa (c) Compressive strength = 95 MPa

Figure 7-6: Comparison of the load-deflection Responses for SFRC (Elsaigh and Kearsley, 2006).

It can be deduced that higher steel fibre contents are necessary for higher strength concrete in order to benefit the most from using steel fibres. This is necessary to ensure that sufficient steel fibres are provided across the crack thus the tensile strength is adequate to sustain the entire or some of peak load in the post-cracking stage. For high strength concrete, steel fibres with a high tensile strength should perform better than steel fibres with a lower tensile strength. On the other hand, adding higher (higher than the optimum) steel fibre contents to normal strength concrete will make little difference.

### 7.5 Effect of changing support stiffness

The support materials G6 and G9 were used in the analysis (refer to Table 7-1). The material model for the SFRC containing 15 kg/m$^3$ was used and kept unchanged (refer to Figure 7-7). The slab thickness used in these analyses is 100 mm.

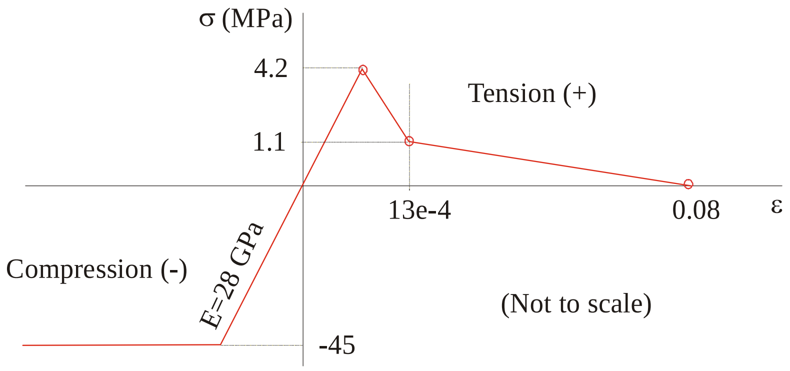


Figure 7-7: Stress-strain curves for SFRC used to study the effect of the support stiffness.

Figure 7-8 indicates that increasing the support stiffness significantly increases the load-carrying capacity of the SFRC ground slab. It also reduces vertical displacements for equal loads. For example, at a displacement of approximately 4 mm in the *P-Δ* responses, the load is increased by approximately 30 percent due to an increase of three times in the stiffness of the support (Young's modulus increased from 50 MPa to 150 MPa). This is similar to the effect obtained by increasing the strength of the SFRC (refer to Figure 7-3). However, increasing the strength of the SFRC is found to provide higher load-carrying capacity compared to increasing the support stiffness.

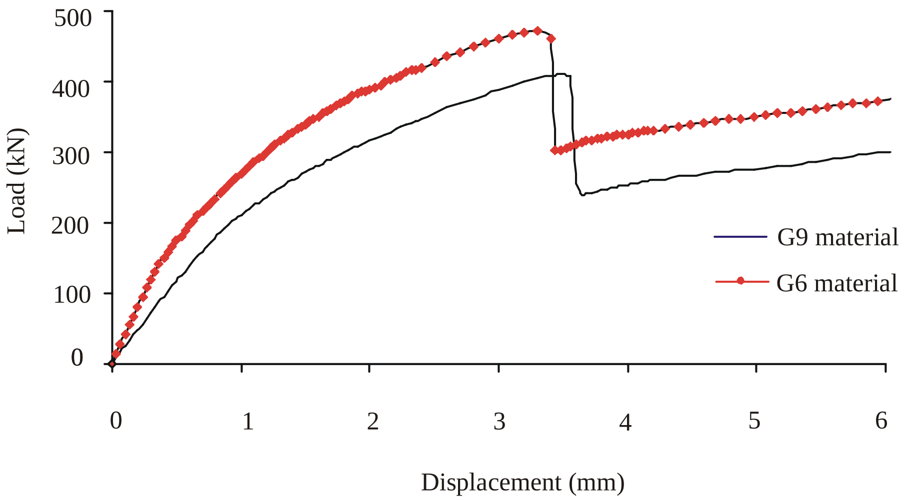


Figure 7-8: Effect of changing support stiffness on the load-displacement responses.

### 7.6 Effect of slab thickness

Based on the trends shown in section 7.3, section 7.4 and section 7.5, a potential for ultra-thin SFRC pavements exists. This can be achieved by adding high steel fibre contents to high strength concrete. Adding too little steel fibres cause little or no improvement to the behaviour of concrete (refer to Figure 7-6(c)). Adding too much steel fibre can be wasteful while reducing the workability of the SFRC. A support material having a relatively high stiffness is also required. In this analysis two support materials and two SFRC materials were used. The materials C2 and G5 having a relatively high stiffness were used for the support (refer to Table 7-1).

Figure 7-9 shows the $\sigma$-$\varepsilon$ responses assumed for the analysis. Both $\sigma$-$\varepsilon$ curves represent an assumed SFRC made of high strength concrete and contain high steel fibre content. The Young's modulus of the SFRC is fairly estimated based on the cube strength of concrete (Holcim Material Handbook, 2006). The cracking strength is assumed as 10 percent of the cube strength. The residual strength is estimated as 90 percent of cracking strength. The thickness of the SFRC is chosen to be 50 mm. These values were assumed arbitrarily.

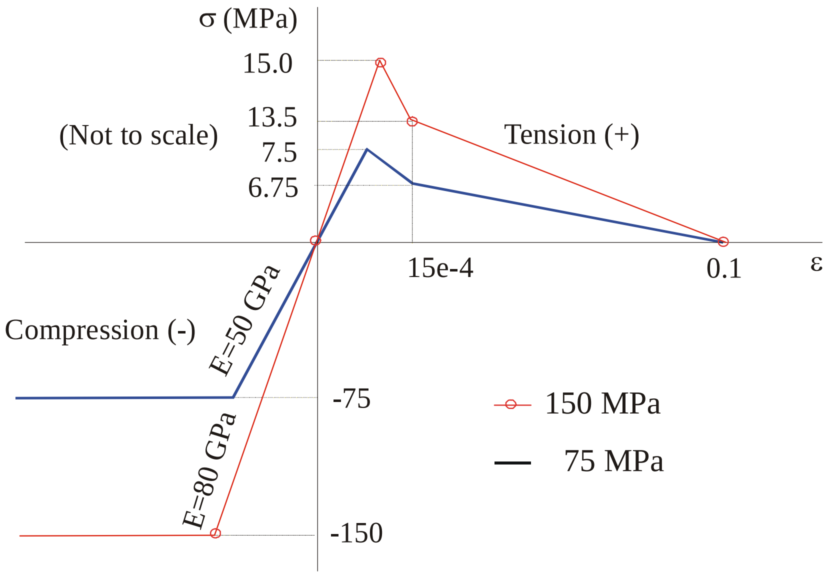


Figure 7-9: Stress-strain curves for SFRC used to study the effect of slab thickness.

Figure 7-10 shows the *P*-*Δ* responses calculated for a relatively thin SFRC ground slab. Comparing Figure 7-10 a and b, the load-carrying capacity of a 50 mm thick SFRC slab can be increased by approximately three times by doubling the strength of the concrete, the support stiffness and using a high steel fibre content. The influence of the support stiffness is greater for higher strength concrete than for lower strength concrete. The trends shown here indicate that ultra-thin slabs can be designed by manipulating the strength of concrete, the steel fibre content and the support stiffness. The appropriate steel fibre content for a particular high strength concrete will need to be a subject for further research.

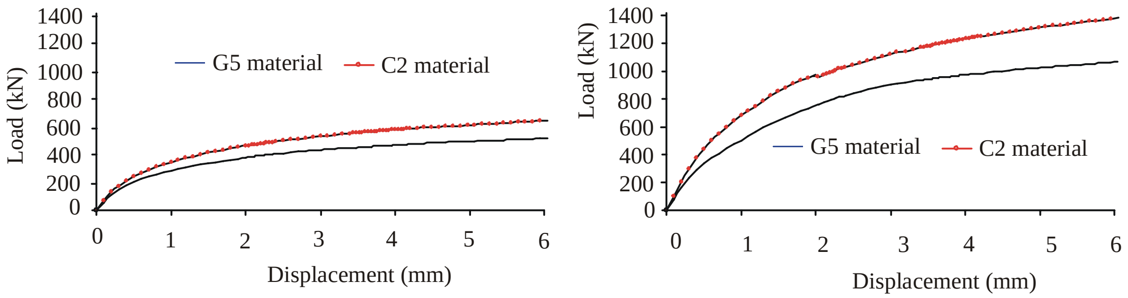


(a) Concrete compressive strength = 75 MPa (b) Concrete compressive strength = 150 MPa

Figure 7-10: The load-displacement responses for thin SFRC ground slabs.

## 7.7 Summary and remarks on the parameter study on the SFRC ground slabs

Increasing the strength of concrete and the steel fibre content increases the load-carrying capacity of the SFRC ground slabs. The increase due to concrete strength is larger than the increase due to steel fibre content. The influence of the steel fibre content is not only dependent on the steel fibre parameters but also dependent on the strength of concrete. An optimum steel fibre content exists for different concrete strengths.

Increasing the support stiffness increases the load-carrying capacity of the SFRC ground slabs. The increase is higher for higher strength concrete than for lower strength concrete. Increasing the strength of concrete results in a larger increase in the load-carrying capacity compared to increasing the support stiffness.

Theoretically an ultra-thin SFRC ground slab can be designed. This can be achieved by providing a relatively hard support, using high strength concrete and optimum steel fibre content. An economic design can be worked out by manipulating these three components.

# CHAPTER 8

# CONCLUSIONS AND RECOMMENDATIONS

## 8.1 Conclusions

The most significant influence of the addition of steel fibres in concrete is to delay and control the tensile cracking of the composite material. This improves the flexural behaviour and increases the post-cracking strength of the SFRC. The post-cracking strength is especially useful for SFRC ground slabs where hinges can form and redistribution of stresses can occur and the load-carrying capacity can thus be increased. SFRC pavements were found to provide superior performance compared to plain concrete and provides equivalent performance compared to conventionally reinforced concrete pavements with equivalent amounts of reinforcement. Existing numerical models used to analyse ground slabs were found inadequate when used for SFRC, as these numerical models do not properly account for the improved mechanical properties of the SFRC. Non-linear finite element analysis can be used to take the post-cracking strength of the SFRC into account thus yielding improved results with respect to actual load-carrying capacity of the slabs. Hence the use of non-linear analyses allows thinner SFRC slabs to be specified compared to the use of existing theories.

The tensile stress-strain ($\sigma$-$\varepsilon$) response for SFRC can be found if either the experimental moment-curvature ($M$-$\phi$) or load-deflection ($P$-$\delta$) responses are available. The proposed method makes use of a small number of assumptions. The major assumption is the shape of the $\sigma$-$\varepsilon$ response. The assumed shape for the $\sigma$-$\varepsilon$ response provided $P$-$\delta$ responses that satisfactorily agreed with experimental results. However, the method can be applied to any selected $\sigma$-$\varepsilon$ response that contains an appropriate number of parameters to model the observed typical $M$-$\phi$ or $P$-$\delta$ behaviour. The merit of the calculation procedure is that it uses measured $M$-$\phi$ or $P$-$\delta$ responses obtainable with minimal testing and measuring complexities compared to stress and strain. The parameter study on SFRC beams highlights the importance of each of the $\sigma$-$\varepsilon$ parameters and shows the manner in which it influences the $M$-$\phi$ or $P$-$\delta$ responses. This information can effectively be used to follow a systematic technique when adjusting $\sigma$-$\varepsilon$ parameters to find a $M$-$\phi$ or $P$-$\delta$ response. The $\sigma$-$\varepsilon$ response calculated using the developed numerical method is mesh size dependent. The area under the softening part of the $\sigma$-$\varepsilon$ response is mostly dependent on the width of the element that lies between the applied loads in the third-point beam test used in the analysis. For finite element analysis, the size of the finite elements should be selected based on this width. However, adjustments to the softening part are necessary if a smaller or larger finite element size is used. The analysis has shown that the point where the material first reaches its maximum tensile stress occurs in the pre-peak regions of both the $M$-$\phi$ and $P$-$\delta$ responses. Hence, the analysis should proceed beyond the cracking stress in order to appropriately evaluate the load-carrying capacity of the SFRC structures.

The calculated $\sigma$-$\varepsilon$ response can be successfully used in non-linear finite element analysis to model the $P$-$\delta$ response of SFRC beams. In the analysis, the input and the output $\sigma$-$\varepsilon$ response extracted at critical integration points match up to a point after which the curves diverge. This can be caused by the numerical simulation used by the finite element software (MSC.Marc) in which the direction of the crack is fixed once the crack initiates (single-fixed crack approach). The actual crack may rotate and the direction of the maximum principal tensile stress changes accordingly. Further analyses using rotating crack approach are recommended to investigate this matter. However, the desired $P$-$\delta$ response was sufficiently calculated up to the limit where the input and the output $\sigma$-$\varepsilon$ response reasonably match.

The calculated tensile $\sigma$-$\varepsilon$ response and the developed finite element model for SFRC slabs can be used to satisfactorily model the behaviour of SFRC ground slabs. The uniaxial $\sigma$-$\varepsilon$ response calculated using the developed numerical method was found sufficient for modelling the biaxial bending response of the analysed SFRC slabs. Thus the assumption that "a crack in a particular direction does not influence the tensile strength of the material parallel to the crack direction" seems to be valid. The validity of this assumption is deduced from the results of various analyses as calculated $P$-$\Delta$ responses using this assumption were found to match the experimental responses. It should be born in mind that several simplifying assumptions were also made in the modelling approach and therefore additional investigation by conducting biaxial tensile tests is recommended. The finite element size should relate to the crack smearing width assumed when calculating the $\sigma$-$\varepsilon$ response. Under the framework of the non-linear finite element analysis, the smeared-cracking approach is found to sufficiently model the cracking behaviour of the SFRC beams and slabs.

A valuable advantage of the developed non-linear finite element model is that it provides the load, the displacement, the crack extent, the tensile strain and the tensile stress on the SFRC slab at any load point on the $P$-$\Delta$ response. The developed finite element model can be used in thickness design of SFRC ground slabs. For a given $\sigma$-$\varepsilon$ response, the finite element model can be used several times to calculate the $P$-$\Delta$ responses for SFRC slabs with different thicknesses. The load-carrying capacity of these SFRC ground slabs can be determined based on the assumed failure limit. The thickness of the slab can be selected depending on the value of the estimated design load.

Increasing the strength of concrete and / or the steel fibre content increases the load-carrying capacity of the SFRC ground slabs. The increase due to concrete strength is larger than the increase due to steel fibre content. The influence of the steel fibre content is not only dependent on the steel fibre parameters but also dependent on the strength of the concrete. This is because of the fibre-matrix behaviour influences the general behaviour of the SFRC slab. Increasing the support stiffness increases the load-carrying capacity of the SFRC ground slabs. The increase is higher for higher strength concrete than for lower strength concrete. Increasing the strength of concrete results in a larger increase in the load-carrying capacity compared to increasing the support stiffness. Theoretically an ultra-thin SFRC ground slab can be designed. This can be achieved by providing a relatively hard support, using high strength concrete and an optimum steel fibre content. An appropriate design can be worked out by manipulating these three components.

## 8.2 Recommendations

The method used to calculate the $\sigma$-$\varepsilon$ response for SFRC is numerically demanding. The numerical solution capabilities of programs such as Mathcad can greatly assist in the implementation of the method. As more measured $P$-$\delta$ responses become available for different concrete strengths and various steel fibre contents, the $\sigma$-$\varepsilon$ responses can be calculated using the Mathcad work sheets. Thereafter, regression analysis can be used to find the relationships between the parameters of the $\sigma$-$\varepsilon$ response. These parameters can be grouped in two equations. The dependent variables can be the compressive strength and the steel fibre content for the two equations respectively. Compared to the use of the Mathcad work sheets, the equations resulting from the regression analysis can lead to less complexities and calculation efforts in finding the $\sigma$-$\varepsilon$ response for SFRC. The parameters (type, strength and dimensions) of steel fibres and the test set up should be kept unchanged for all selected experimental results. The developed regression equations can be used to calculate $\sigma$-$\varepsilon$ responses that relate to the particular steel fibre used and to the element size inherent to the crack smearing width in the beam test. Further research can be conducted to expand the numerical method used to calculate the $\sigma$-$\varepsilon$ response to allow for calculation of the crack width ($w$) at a specific tensile stress or a strain. This will allow the estimation of the $w$ in the SFRC structures. It can be used to decide on the failure of SRFC structures if a $w$ limit is specified. The crack width might be crucial to the durability of the pavement if the SFRC is to be used in regions with severe weather conditions.

Apart from the availability of finite element software, the task of performing non-linear analysis is not practical for many practicing engineers. A practical way is to create design tables that can assist in the design of SFRC ground slabs. The availability of steel fibres with a variety of mechanical and physical properties as well as the use of various fibre contents tend to complicate the creation of such design tables at this stage. However, for specific types of steel fibres and concrete strengths experimental work can be planned to cast SFRC beams having different steel fibre contents. These beams can be tested to generate the $P$-$\delta$ responses and the relevant $\sigma$-$\varepsilon$ response can then be calculated. The developed finite element model can be used. The steel fibre content and the thickness of the SFRC are changed every time. The obtained results can be used to establish a design table for the type of the steel fibre and the concrete strength used.

The developed approach can be successfully used in the analysis and design of SFRC ground slabs subject to interior loading. Further experiments are required to investigate its validity of the edge and corner load cases. Loading caused by mechanical load might not be the only limiting design factor especially for thin SFRC slabs. Thin slabs are thought to generate higher potential for curling and warping. The combined effect of the stresses due to mechanical load and the stresses due to moisture and temperature changes need to be considered. A finite element model can be developed to assess the stresses due to moisture and temperature changes.